

Time and Energy Optimal Control for a Single Track Modeled Vehicle.

Anton Pozharskiy

Albert-Ludwigs-Universität Freiburg
Freiburg, Germany
anton@pozhar.ski

Mario Willaredt

Albert-Ludwigs-Universität Freiburg
Freiburg, Germany
mario-Willaredt@web.de

Adil Younas

Albert-Ludwigs-Universität Freiburg
Freiburg, Germany
adil.younas@gmx.de

Abstract—

Index Terms—Optimal Control, Model Predictive Control, Tire Models, Time Optimal Control.

I. INTRODUCTION

Optimal control has become a popular paradigm of controller design in a multitude of autonomous vehicle projects. There also exists prior work on model predictive control as applied specifically to the target of the project: time optimal planning and control [1] [2]. In this project we attempt to formulate true time optimal controller that takes into account a tire model with slip angles and independent tire forces. Generally optimal control and MPC algorithms must tradeoff the complexity of the dynamic model and speed of the solver. In the past work it is very common for the authors to use simple slip free bicycle model to implement the vehicle dynamics, however there are often interesting behaviors such as countersteer and tire dynamics that are not modeled.

The path planning aspect of the time optimal driving problem provides the primary difficulty of the approach taken in this project, along with the severe nonlinearity introduced not just by the tire model, but also by the commonly used time optimality reformulation that takes the “speed of time” as an optimization variable. This nonlinearity often leads to local minima and makes the problem highly sensitive to initialization and hyperparameters.

II. FORMULATION

A. Dynamics

The model of the dynamic system can be broken up into the road model, the dynamics of the vehicle in the CG (center of gravity) frame, and the dynamics of the vehicle in the curvilinear coordinate system.

1) *Road Model:* The first challenge in formulating a vehicle model is modeling the road surface, which is generally a long narrow strip. This combined with the fact that roads generally do not form convex sets in euclidian space means that a different coordinate system is needed. For this purpose a curvilinear coordinate system is used. In this model the vehicle’s position is represented by the distance along the center-line of the road (s), the distance perpendicular to the centerline (n), and the relative angle α to the direction of the road. The road’s position in euclidean space is defined as in [2], i.e. a normalized parametric curve which is defined by a single function $\kappa(s)$ which defines the rate of change which gives us the road centerline coordinates as:

$$x' = \cos(\theta) \quad (1a)$$

$$y' = \sin(\theta) \quad (1b)$$

$$\theta' = \kappa(s) \quad (1c)$$

The (s, n, α) coordinate system is right handed as shown in Figure. (TODO). With this formulation the road is fully defined with the addition of a formalism for the road edges. The problem formulation addressed by ACADOS limits us to a single width function $w(s)$, which defines the symmetric edges of the road w_r, w_l :

$$w_r = -w(s) \quad (2a)$$

$$w_l = w(s) \quad (2b)$$

2) *CG Dynamics:* The CG dynamics of the vehicle is modeled using a bicycle model (Figure. 14) that takes into account the slip angles and forces exerted by the front and rear tires independently.

The state space of the CG dynamics is as follows:

$$x_{cg} = \begin{bmatrix} u \\ v \\ \omega \\ \delta \end{bmatrix} \quad (3)$$

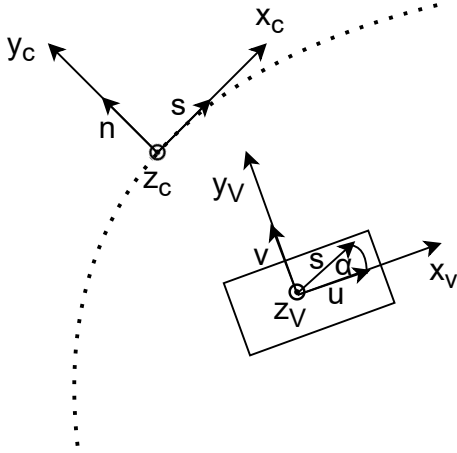


Fig. 1. curvilinear coordinate system

The model has three degrees of freedom that are used as control variables: the brake torque τ_b , the brake torque τ_e , and the steering rate ω_{steer} :

$$u = \begin{bmatrix} \tau_b \\ \tau_e \\ \omega_{\text{steer}} \end{bmatrix} \quad (4)$$

The vehicle is modeled as rear wheel drive only. Each tire experiences two forces transverse and parallel to the rolling axis of the tire as shown in Figure. 2 The parallel forces are defined as follows:

$$F_{fp} = -k_b \tau_b \quad (5a)$$

$$F_{rp} = k_e \tau_e - k_b \tau_b \quad (5b)$$

The transverse forces are modeled as a linear w.r.t the slip angle of the tire. The direction of travel angles are defined as follows:

$$\tan \gamma_r = \frac{v - l_r \omega}{u} \quad (6a)$$

$$\tan \gamma_f = \frac{v + l_f \omega}{u} \quad (6b)$$

and the slip angles are:

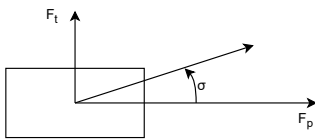


Fig. 2. Forces acting on a tire.

$$\sigma_r = \gamma_r \quad (7a)$$

$$\sigma_f = \gamma_f - \delta \quad (7b)$$

the forces are then linear w.r.t the slip angles:

$$F_{ft} = -K_f \sigma_f N_f \quad (8a)$$

$$F_{rt} = -K_r \sigma_r N_r \quad (8b)$$

with N_f and N_r being the normal force on the tire in the front and rear respectively.

The dynamics in the CG frame is then simply defined through simple euclidean kinematics:

$$\dot{x}_{cg} = \begin{bmatrix} F_{rp} + F_{fp} \cos \delta - F_{ft} \sin \delta \\ F_{rf} + F_{fp} \sin \delta + F_{ft} \cos \delta \\ -l_r F_{rt} + l_f (F_{ft} \cos \delta + F_{fp} \sin \delta) \\ \omega_{\text{steer}} \end{bmatrix} \quad (9)$$

3) *Vehicle Dynamics*: The dynamics of the vehicle in the curvilinear frame can be entirely separated from the CG dynamics as long as the CG dynamics provide u , v , and ω . The state of the system in the curvilinear state is:

$$x_{\text{curv}} = \begin{bmatrix} s \\ n \\ \alpha \end{bmatrix} \quad (10)$$

Given these states we can define the dynamics:

$$\dot{x}_{\text{curv}} = \begin{bmatrix} \frac{u \cos \alpha - v \sin \alpha}{1 - n \kappa(s)} \\ u \sin \alpha + v \cos \alpha \\ \omega - \kappa(s) \frac{u \cos \alpha - v \sin \alpha}{1 - n \kappa(s)} \end{bmatrix} \quad (11)$$

With these dynamics defined the dynamics of the whole system are defined as:

$$x_{\text{dyn}} = \begin{bmatrix} x_{\text{curv}} \\ x_{cg} \end{bmatrix} \quad (12a)$$

$$\dot{x}_{\text{dyn}} = \begin{bmatrix} \dot{x}_{\text{curv}} \\ \dot{x}_{cg} \end{bmatrix} \quad (12b)$$

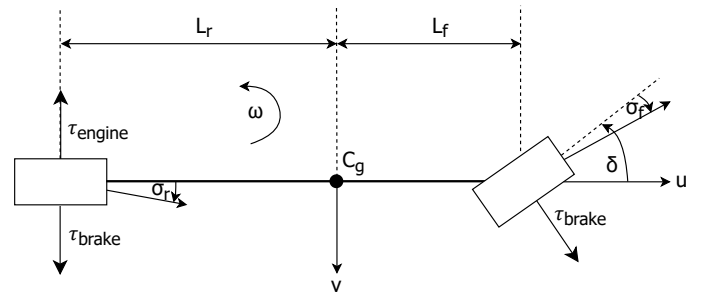


Fig. 3. CG coordinate system

B. Problem Formulation

The MPC problem is solved using the ACADOS tool [3], which treats a specific problem formulation. In order to formulate the time optimal problem, a new state Δ_t is introduced that represents the speed of time. This gives the normalized dynamics:

$$x_{\text{topt}} = \begin{bmatrix} x_{\text{curv}} \\ \Delta_t \\ x_{\text{cg}} \end{bmatrix} \quad (13a)$$

$$\dot{x}_{\text{topt}} = \Delta_t \begin{bmatrix} \dot{x}_{\text{curv}} \\ 0 \\ \dot{x}_{\text{cg}} \end{bmatrix} \quad (13b)$$

These dynamics are reformulated into implicit dynamics in order to use the implicit Runge-Kutta methods provided in ACADOS:

$$f_{\text{impl}}(x_{\text{topt}}, \dot{x}_{\text{topt}}, u) = \dot{x}_{\text{topt}} - \Delta_t \begin{bmatrix} \dot{x}_{\text{curv}} \\ 0 \\ \dot{x}_{\text{cg}} \end{bmatrix} \quad (14)$$

This then gives us the following formulation of the optimal control problem:

$$\begin{aligned} \min_{x_{\text{topt}}(\cdot), u(\cdot)} \int_0^1 & \Delta_t^2 + 10^{-6} \tau_e \tau_b \\ & + 10^{-6} \tau_e^2 \\ & + 10^{-6} \tau_b^2 \\ & + 10^{-6} \omega_{\text{steer}}^2 \end{aligned} \quad (15a)$$

subject to the equality constraints with τ dependence dropped where convenient:

$$f_{\text{impl}}(x_{\text{topt}}, \dot{x}_{\text{topt}}, u) = 0 \quad \tau \in (0, 1] \quad (15b)$$

$$x_{\text{curv}}(0) = x_{\text{curv}0} \quad (15c)$$

$$x_{\text{cg}}(0) = x_{\text{cg}0} \quad (15d)$$

$$s(1) = s_{\text{max}} \quad (15e)$$

And the inequality constraints:

$$0 \leq \Delta_t(0) \leq 3 \quad (15f)$$

$$-1 \leq \frac{n(\tau)}{w(s(\tau))} \leq 1 \quad \tau \in (0, 1) \quad (15g)$$

$$-\frac{\pi}{2} \leq \alpha(\tau) \leq \frac{\pi}{2} \quad \tau \in (0, 1) \quad (15h)$$

$$-\frac{\pi}{4} \leq \delta(\tau) \leq \frac{\pi}{4} \quad \tau \in (0, 1) \quad (15i)$$

$$0 \leq \tau_e(\tau) \leq 1 \quad \tau \in (0, 1) \quad (15j)$$

$$0 \leq \tau_b(\tau) \leq 1 \quad \tau \in (0, 1) \quad (15k)$$

$$-0.5 \leq \omega_{\text{steer}}(\tau) \leq 0.5 \quad \tau \in (0, 1) \quad (15l)$$

$$F_{rp}^2 + F_{rt}^2 \leq (\mu N_r)^2 \quad \tau \in (0, 1) \quad (15m)$$

$$F_{fp}^2 + F_{ft}^2 \leq (\mu N_f)^2 \quad \tau \in (0, 1) \quad (15n)$$

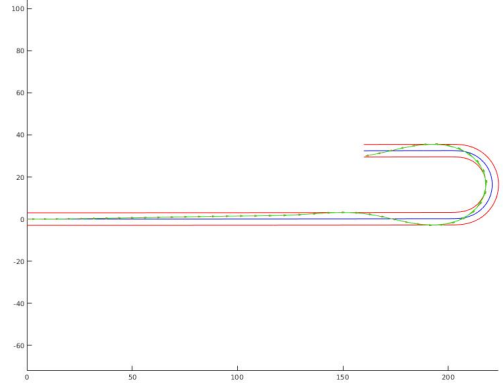


Fig. 4. Trajectory followed by the vehicle in the high speed hairpin experiment.

The primary cost in Equation. (15a) is the square of the speed of time variable Δ_t . This enforces the time optimality target of the optimal control problem. The cross term $\tau_e \tau_b$ is introduced to minimize application of engine torque and brakes at the same time, and the remaining cost terms are to enforce minimality of control inputs. Equation (15b) is the dynamics of the system, Equations (15c), (15d), and (15f) set the initial conditions of the system including range of values that the free variable of Δ_t can take. The remaining inequalities represent the physical limits of the system. In particular the last two inequalities are crucial to realistic modeling of the vehicle and provide the grip limits of the tires, similarly to the approach taken in [2].

In order to improve the convergence properties we introduce slack variables with L_1 penalties to the inequalities in Equations (15g), (15m), and (15n).

III. NUMERICAL SOLUTION

A. Solver Options

The problem formulated above is solved using the ACADOS package. Due to inconsistency in convergence behavior from problem instance to problem instance some parameters were tuned specifically to get convergent results. These will be discussed in the conclusions and further explorations sections of this report. However there were several consistent parameters that were used for all the following experiments.

Contant	Value
m	1440 kg
I	1730 kgm ²
l_f	1.482 m
l_r	1.118 m
k_e	10 ⁴
k_b	2 × 10 ⁴
b_b	0.5
m_b	0.5
K_r	29
K_f	29
C_u	0.039 $\frac{Ns^2}{m^2}$
C_v	0.039 $\frac{Ns^2}{m^2}$
μ	1.2

TABLE I
VEHICLE CONSTANTS

The dynamics are discretized using a 4th order implicit Runge-Kutta method with $N = 50$. Globalization is done through the merit function backtracking feature provided in the ACADOS package, using default settings. The required stopping tolerances for stationarity and inequality are set to 10^{-4} and 10^{-5} respectively. The problem is then solved using the standard SQP (sequential quadratic programming) approach (the real time iteration approach will be discussed in the Conclusions section). The QPs formed in the SQP method are solved using the partial condensing HPIPM [4] method.

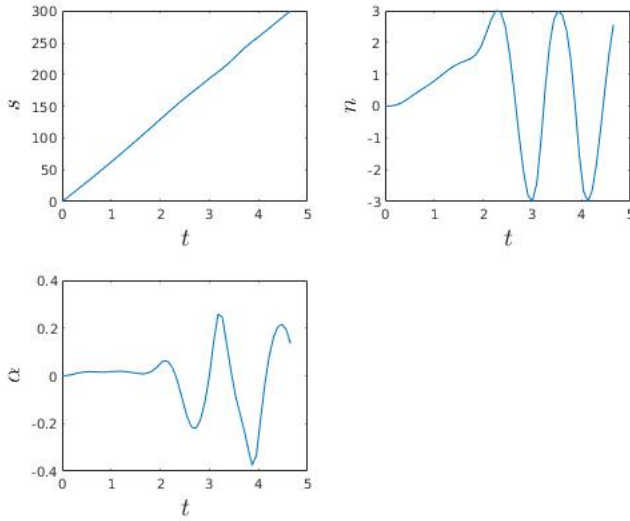


Fig. 5. Curvilinear coordinates of vehicle in the high speed hairpin experiment.

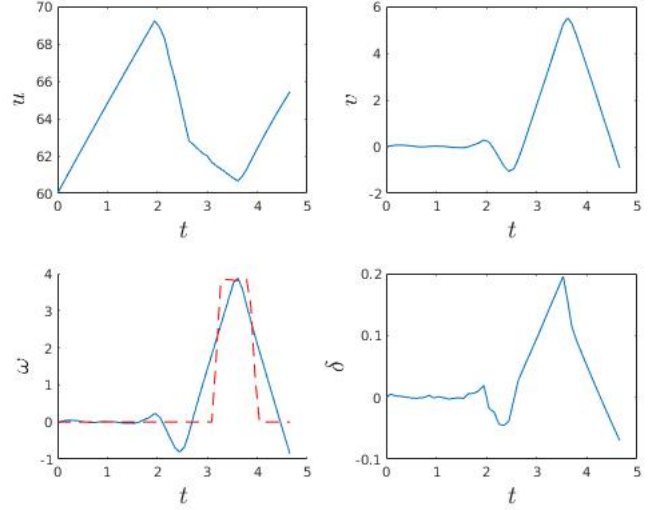


Fig. 6. Center of gravity dynamics of the vehicle in the high speed hairpin experiment.

B. Initialization and Warm Starting

Initialization of the ACADOS solver plays a very important role in the convergence behavior of the controller. In this case the apriori knowledge of the curvature of the road is used in order to initialize ω , δ , and ω_{steer} . The remaining state variables are initialized through simple linear interpolation. As the problem solves time domain optimization, there is a risk if s_{max} is too small then the resulting Δt may be too small and would overestimate the capability of the vehicle. As such s_{max} is iterated via

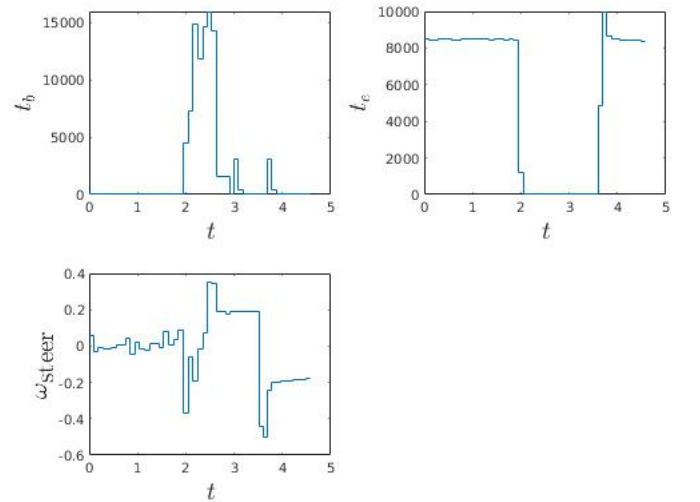


Fig. 7. Controls in the high speed hairpin experiment.

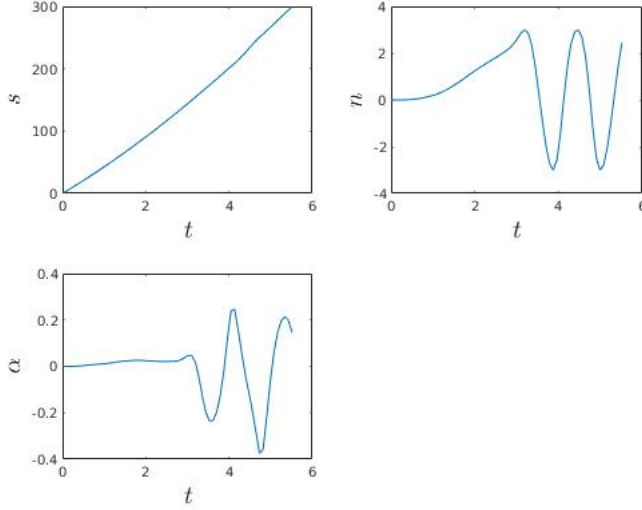


Fig. 8. Curvilinear coordinates of vehicle in the low speed hairpin experiment.

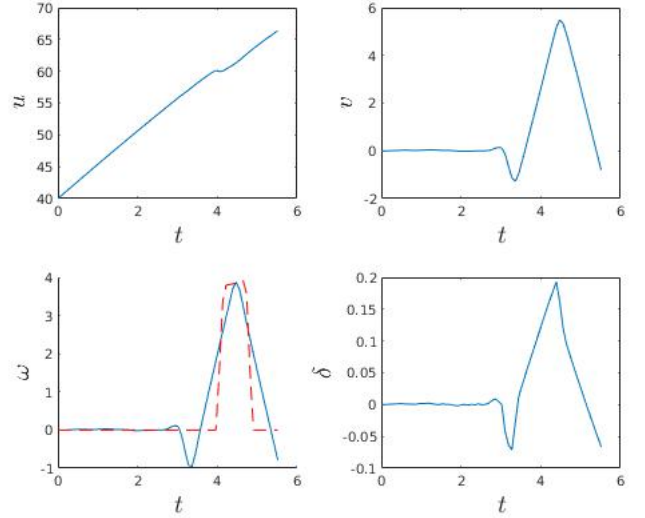


Fig. 9. Center of gravity dynamics of the vehicle in the low speed hairpin experiment.

a constant target Δ_t (in the case of the below experiments $\Delta_t = 0.1$) and $s_{\max, i+1} = s_i + N\Delta_t u_i$ to approximate distance traveled at a constant speed in time $N\Delta_t$.

Warm starting is done via a simple shift in the old control and state solutions and then the addition of a final state with $s = s_{\max}$. This warmstarting improves the convergence of the optimization routine but also may cause issues with local minima in particularly difficult corners, which even the existing globalization algorithm fails to recover from when those solutions disappear.

IV. RESULTS

A. Experimental Setup

Several experiments were run to evaluate the behavior of the MPC controller corresponding to several common corner types. The vehicle modeled is similar to the one described in [2]. The Vehicle constants are listed in Table. TODO.

B. Experiments

1) *Hairpin*: The first sort of turn tested is the so called “hairpin” turn, i.e. a 180 degree turn with a small radius of curvature, in this case a radius of approximately 15 meters. Two experiments were run, in the first the vehicle approaches the turn at a relatively slow speed of 40 meters per second and does not need to slow down to make the turn, and in the second experiment the vehicle approaches the turn at speed of 60 meters per second and must brake in order to stay on the road and make the turn.

As shown in the resulting plots the controller successfully navigates a situation where it must slow down to traverse the track in a time optimal way. The controller also takes the path through the turn with the highest radius, minimizing the need for braking and optimizing exit speed for the following straight. The low speed experiment also shows an interesting behavior where the controller stops accelerating momentarily at the highest curvature point in order to maintain tire grip.

For this scenario the no regularization method is used,

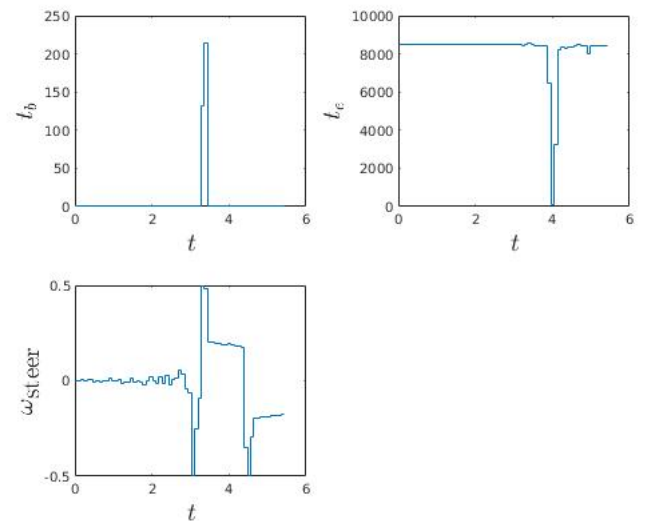


Fig. 10. Controls in the low speed hairpin experiment.

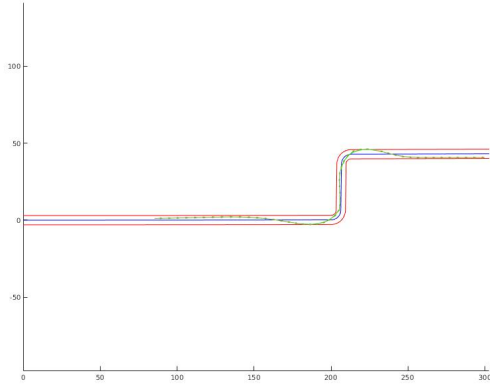


Fig. 11. Trajectory followed by the vehicle in the chicane experiment.

and Levenberg-Marquardt constant of 0.01.

2) *Chicane*: A further interesting experiment which was run was a squared off “street circuit” style chicane with two 90 degree turns, set 30 meters apart. Again the vehicle is forced to slow down to maintain tire grip. This experiment required significant tuning and was extremely sensitive to changes in chicane length and initial vehicle velocity. For this scenario the ‘convexify’ regularization method is used, along with a higher Levenberg-Marquardt constant of 0.1.

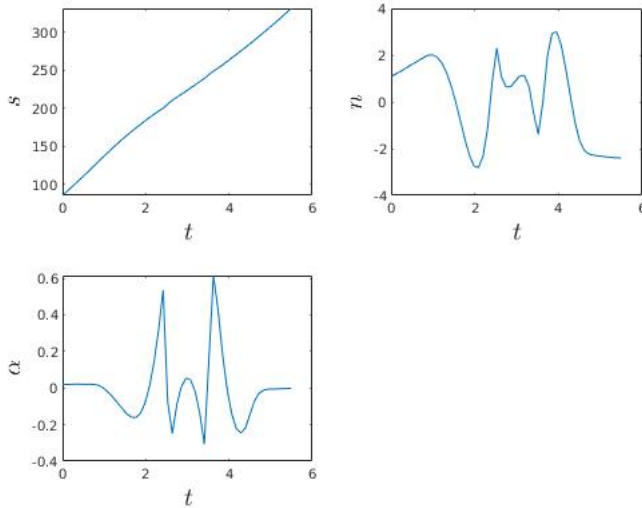


Fig. 12. Curvilinear coordinates of vehicle in the chicane experiment.

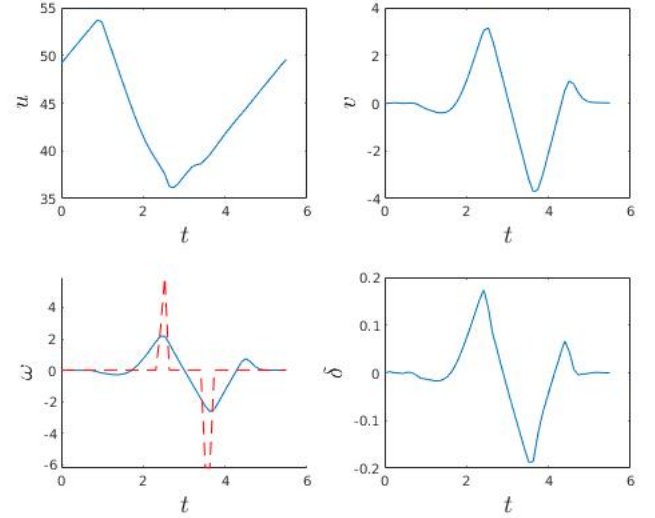


Fig. 13. Center of gravity dynamics of the vehicle in the chicane experiment.

It is useful to note that in all 3 of these examples the cross term for engine and brake application perform the desired purpose and prevent brake and throttle application at the same time.

Unfortunately in its current implementation, this controller runs at approximately 25 times slower than real time when used in ordinary SQP mode. This is primarily due to the prevalence of steps in which the solver never reaches the required tolerances, that with the 1000 maximum iterations take multiple seconds to

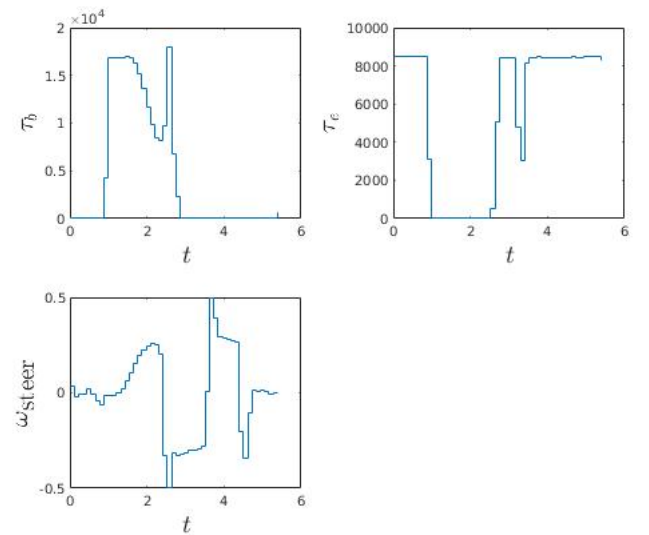


Fig. 14. Controls in the high speed hairpin experiment.

complete. The authors could not manage to successfully get convergence of the real time iteration even with initialization via pre solving a single SQP.

V. CONCLUSIONS

This project has only partially achieved it's goal of a robust time optimal model predictive controller. On one hand the formulation of the problem has successfully been proven out as viable. On the other hand tuning requirements specific to each scenario means that the system is not sufficiently general to operate on an actual track, or when significant model-plant mismatches exist. Once tuned the controller does however produce excellent results in difficult situations that require complex maneuvers and operates in a time optimal fashion while maintaining the physical constraints of the vehicle.

VI. FURTHER EXPLORATION

There are several possible paths for extension to this project. The need to possibly re-formulate constraints or take advantage of other tricks to improve convergence, is a necessity. Further exploration of nonlinear tire models would also be interesting, in particular the use of a non-smooth model instead of the oft used "magic formula" [5], to take advantage of advancements in non-smooth solvers.

REFERENCES

- [1] R. Verschueren, S. D. Bruyne, M. Zanon, J. V. Frasch, and M. Diehl, "Towards time-optimal race car driving using nonlinear MPC in real-time," in *Proceedings of the IEEE Conference on Decision and Control (CDC)*, 2014, pp. 2505–2510.
- [2] R. Lot and F. Biral, "A curvilinear abscissa approach for the lap time optimization of racing vehicles," *IFAC Proceedings Volumes*, vol. 47, no. 3, pp. 7559–7565, 2014, 19th IFAC World Congress.
- [3] R. Verschueren, G. Frison, D. Kouzoupis, J. Frey, N. van Duijkeren, A. Zanelli, B. Novoselnik, T. Albin, R. Quirynen, and M. Diehl, "acados – a modular open-source framework for fast embedded optimal control," *Mathematical Programming Computation*, Oct 2021. [Online]. Available: <https://doi.org/10.1007/s12532-021-00208-8>
- [4] G. Frison and M. Diehl, "Hpipm: a high-performance quadratic programming framework for model predictive control," 2020. [Online]. Available: <https://arxiv.org/abs/2003.02547>
- [5] J. P. Pauwelussen, "Chapter seven - exercises," in *Essentials of Vehicle Dynamics*, J. P. Pauwelussen, Ed. Oxford: Butterworth-Heinemann, 2015, pp. 239–255.